Article

Multipurpose Organically Modified Carbon Nanotubes: From Functionalization to Nanotube Composites

Vasilios Georgakilas, Athanasios Bourlinos, Dimitrios Gournis, Theodoros Tsoufis, Christos Trapalis, Aurelio Mateo-Alonso, and Maurizio Prato

J. Am. Chem. Soc., **2008**, 130 (27), 8733-8740 • DOI: 10.1021/ja8002952 • Publication Date (Web): 14 June 2008

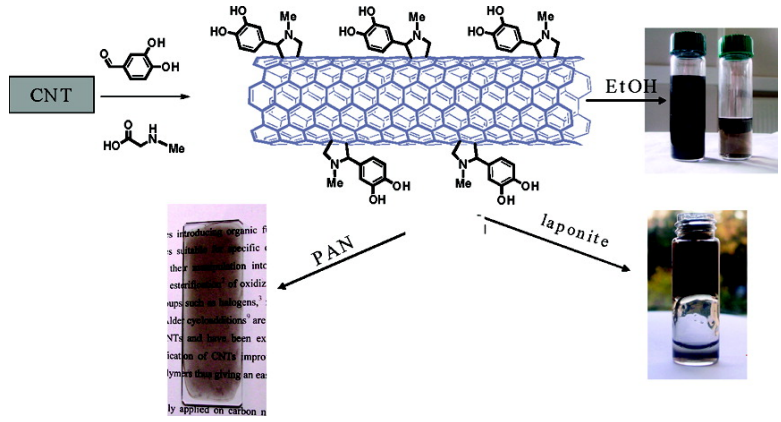

J|A|C|S
ARTICLES

Published on Web 06/14/2008

Multipurpose Organically Modified Carbon Nanotubes: From Functionalization to Nanotube Composites

Vasilios Georgakilas,*,† Athanasios Bourlinos,† Dimitrios Gournis,‡ Theodoros Tsoufis,‡ Christos Trapalis,† Aurelio Mateo-Alonso,§ and Maurizio Prato*,§

Institute of Materials Science, N.C.S.R. "Demokritos", GR-15310 Agia Paraskevi Athens, Greece, Department of Materials Science and Engineering, University of Ioannina, GR-45110 Ioannina, Greece, and Center of Excellence for Nanostructured Materials (CENMAT), Dipartimento di Scienze Farmaceutiche, INSTM, Universita di Trieste, Piazzale Europa 1, 34127 Trieste, Italy

Received January 14, 2008; E-mail: georgaki@ims.demokritos.gr; prato@units.it

Abstract: We show that covalent functionalization of carbon nanotubes (CNTs) via 1,3-dipolar cycloaddition is a powerful method for enhancing the ability to process CNTs and facilitating the preparation of hybrid composites, which is achieved solely by mixing. CNTs were functionalized with phenol groups, providing stable dispersions in a range of polar solvents, including water. Additionally, the functionalized CNTs could easily be combined with polymers and layered aluminosilicate clay minerals to give homogeneous, coherent, transparent CNT thin films and gels.

Introduction

Carbon nanotubes (CNTs) constitute a promising material for use in the aerospace, textile, and electronics industries, since this material possesses high chemical and thermal stability, mechanical strength, flexibility, and electrical and thermal conductivity as well as low weight.[1] As a matter of fact, the combination of all of these properties in a single material has increased the interest in implementing CNTs in current technology. In particular, the electronic properties of CNTs in homogeneous and transparent CNT thin-film composites are currently being evaluated for applications in electronic devices such as smart windows, light-emitting diodes, solar cells.[1,2] Incorporation of even small amounts of CNTs in other materials[3] can improve their mechanical stabilities[3c,4a,b] and thermal and electrical properties.[4c]

A major drawback in the use of CNTs is the difficulty of processing them, as they are immiscible with most media because of their great tendency to establish strong van der Waals and $\pi-\pi$ interactions, which cause them to form tight bundles. Hence, when mixed with other components, CNTs tend to segregate by self-aggregation, which hinders the development of homogeneity and does not allow (or at least complicates) the preparation of the composite. An essential aspect of future commercial applications is that CNTs should be compatible with other components with respect to formation of homogeneous composites as well as easy to manipulate and process.[2a]

Chemical modification of CNTs improves their dispersibility in organic solvents and water and makes them more compatible with other materials, facilitating the preparation of composites.[5] Functionalization not only facilitates CNT manipulation by various processes (mixing, blending, dispersion) but also allows

† N.C.S.R. "Demokritos".
‡ University of Ioannina.
§ Universita di Trieste.

(1) (a) Coleman, J. N.; Khan, U.; Blau, W. J.; Gunko, Y. K. *Carbon* **2006**, *44*, 1624–1652. (b) Baughman, R. H.; Zakhidov, A. A.; Heer, W. A. *Science* **2002**, *297*, 787–792. (c) Wu, Z.; Chen, Z.; Du, X.; Logan, J. M.; Sippel, J.; Nikolou, M.; Kamaras, K.; Reynolds, J. R.; Tanner, D. B.; Hebard, A. F.; Rinzler, A. G. *Science* **2004**, *305*, 1273–1276. (d) Artukovic, E.; Kaempgen, M.; Hecht, D. S.; Roth, S.; Gruner, G. *Nano Lett.* **2005**, *5*, 757–760. (e) Bekyarova, E.; Itkis, M. E.; Cabrera, N.; Zhao, B.; Yu, A.; Gao, J.; Haddon, R. C. *J. Am. Chem. Soc.* **2005**, *127*, 5990–5995. (f) White, C. T.; Todorov, T. N. *Nature* **1998**, *393*, 240–242. (g) Zhang, M.; Fang, S.; Zakhidov, A. A.; Lee, S. B.; Aliev, A. E.; Williams, C. D. *Science* **2005**, *309*, 1215–1219.

(2) (a) Gruner, G. *J. Mater. Chem.* **2006**, *16*, 3533–3539. (b) Sgobba, V.; Guldi, D. M. *J. Mater. Chem.* **2008**, *18*, 153–157. (c) Guldi, D. M.; Rahman, G. M. A.; Zerbetto, F.; Prato, M. *Acc. Chem. Res.* **2005**, *38*, 871–878. (d) Kim, D. K.; Lee, M. H.; Lee, J. H.; Lee, T. W.; Kim, K. J.; Lee, Y. K.; Kim, T.; Choi, H. R.; Koo, J. C.; Nam, J. D. *Org. Electron.* **2008**, *9*, 1–13. (e) Ferrer-Anglada, N.; Kaempgen, M.; Skakalova, V.; Dettlaf-Weglikowskab, U.; Roth, S. *Diamond Relat. Mater.* **2004**, *13*, 256–260.

(3) (a) Yao, Z.; Braidy, N.; Botton, G. A.; Adronov, A. *J. Am. Chem. Soc.* **2003**, *125*, 16015–16024. (b) Liu, L. Q.; Tasis, D.; Prato, M.; Wagner, H. D. *Adv. Mater.* **2007**, *19*, 1228–1233. (c) Saeed, K; Park, S. Y. *J. Appl. Polym. Sci.* **2007**, *106*, 3729–3735. (d) Kashiwagi, T.; Du, F.; Douglas, J. F.; Winey, K. I.; Harris, R. H., Jr.; Shields, J. R. *Nat. Mater.* **2005**, *4*, 928–933.

(4) (a) Zhang, W. D.; Phang, I. Y.; Liu, T. X. *Adv. Mater.* **2006**, *18*, 73–77. (b) Litina, K.; Miriouni, A.; Gournis, D.; Karakassides, M. A.; Georgiou, N.; Klontzas, E.; Ntoukas, E.; Avgeropoulos, A. *Eur. Polym. J.* **2006**, *42*, 2098–2107. (c) Liu, L.; Grunlan, J. C. *Adv. Funct. Mater.* **2007**, *17*, 2343–2348. (d) Costache, M. C.; Heidecker, M. J.; Manias, E.; Camino, G.; Frache, A.; Beyer, G.; Gupta, R. K.; Wilkie, C. A. *Polymer* **2007**, *42*, 6532–6545.

(5) (a) Hirsch, A.; Vostrowsky, O. *Top. Curr. Chem.* **2005**, *245*, 193–237. (b) Balasubramanian, K.; Burghard, M. *Small* **2005**, *1*, 180–192. (c) Banerjee, S.; Kahn, M. G. C.; Wong, S. S. *Chem.—Eur. J.* **2003**, *9*, 1898–1908. (d) Niyogi, S.; Hamon, M. A.; Hu, H.; Zhao, B.; Bhowmik, P.; Sen, R.; Itkis, M. E.; Haddon, R. C. *Acc. Chem. Res.* **2002**, *35*, 1105–1113. (e) Tasis, D.; Tagmatarchis, N.; Bianco, A.; Prato, M. *Chem. Rev.* **2006**, *106*, 1105–1136.

Scheme 1. (left) Schematic Representation of 1,3 Dipolar Cycloaddition to CNTs Using 3,4-Dihydroxybenzaldehyde and (right) Photograph of a Solution of SWCNT-*f*-OH in DMF.

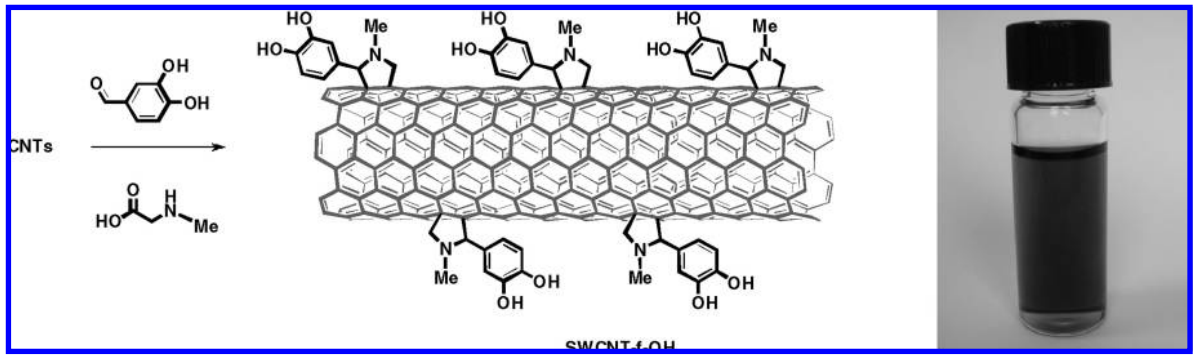

tuning of their chemical and physical properties for specific demands and upgrades their quality through effective purification.[6]

In this work, we show that covalent functionalization of CNTs is a powerful tool for enhancing the ability to process CNTs and facilitating the preparation of homogeneous composites with polymers or clays. CNTs were functionalized with phenol groups via 1,3-dipolar cycloaddition[7] in a single step using commercially available reagents. Sidewall functionalization provided stable dispersions of CNTs in a range of polar solvents, including water, allowing the fabrication of composites by mixing the components in solution at room temperature. In fact, the functionalized CNTs were found to be compatible with polymers or layered aluminosilicate clay minerals, giving homogeneous, coherent, transparent CNT thin films and/or gels.

Functionalization of CNTs

Initially, the 1,3-dipolar cycloaddition was tested on single-walled CNTs (SWCNTs), since the degree of functionalization is easier to assess and well-established characterization protocols exist in this case.[8] The reaction was carried out using *N*-methylglycine and 3,4-dihydroxybenzaldehyde (Scheme 1, left), both of which are commercially available and affordable. After the reaction, most of the physically adsorbed organic materials were removed by filtration (see the Experimental Section). The introduction of phenolic substituents makes the nanotubes more compatible with other solvents, rendering them dispersibile in dimethylformamide (DMF) (0.2 mg mL^{-1}), for example (Scheme 1, right). The resulting hydroxyl-functionalized SWCNT material (SWCNT-*f*-OH) was characterized by Raman spectroscopy, thermal gravimetric analysis (TGA), transmission electron microscopy (TEM), and atomic force microscopy (AFM), all of which confirmed that the reaction had taken place, affording the desired SWCNT-*f*-OH.

The functionalization was evidenced by Raman spectroscopy (Figure 1). Comparison of the Raman spectra of neat SWCNTs and SWCNT-*f*-OH showed that the ratio of G- ($\sim$1600 cm^{-1}) and D-band ($\sim$1300 cm^{-1}) intensities (the I_G/I_D ratio) was reduced significantly (from 28 in the pristine SWCNTs to 10 for SWCNT-*f*-OH). This decrease was caused by the change in hybridization of the carbon atoms from sp^2 to sp^3 due to cycloaddition on the sidewalls and tips of the nanotubes. This is currently considered the most compelling evidence for covalent functionalization of SWCNTs.[8]

The UV−vis−near-infrared (NIR) spectrum of a saturated SWCNT-*f*-OH dispersion in DMF is shown in Figure 2. The features in the spectrum are due to the van Hove singularities of metallic and semiconducting nanotubes and were attributed to their band-gap transitions. The width of these features reflect the overlap of features from CNTs having different diameters and chiral indices.

TEM and AFM characterization gave direct proof of the presence of functionalized SWCNTs. Representative images

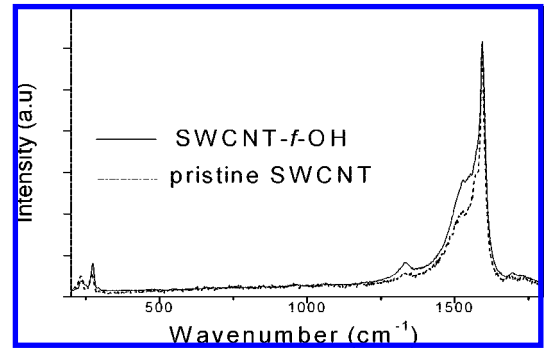

Figure 1. Raman spectra of pristine SWCNTs and SWCNT-*f*-OH.

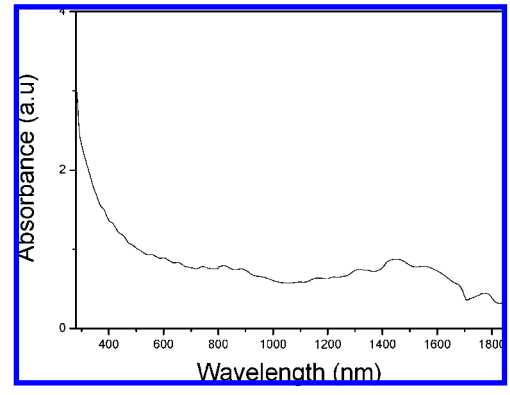

Figure 2. UV−vis−NIR spectrum of a saturated solution of SWCNT-*f*-OH in DMF.

(6) (a) Georgakilas, V.; Voulgaris, D.; Vazquez, E.; Prato, M.; Guldi, D. M.; Kukovecz, A.; Kuzmany, H. *J. Am. Chem. Soc.* **2002**, *124*, 14318–14319. (b) Lovat, V.; Pantarotto, D.; Lagostena, L.; Cacciari, B.; Grandolfo, M.; Righi, M.; Spalluto, G.; Prato, M.; Ballerini, L. *Nano Lett.* **2005**, *5*, 1107–1110.

(7) (a) Georgakilas, V.; Kordatos, K.; Prato, M.; Guldi, D. M.; Holzinger, M.; Hirsch, A. *J. Am. Chem. Soc.* **2002**, *124*, 760–761. (b) Georgakilas, V.; Tagmatarchis, N.; Pantarotto, D.; Bianco, A.; Briand, J.-P.; Prato, M. *Chem. Commun* **2002**, 3050–3051.

(8) (a) Dyke, C. A.; Tour, J. M. *J. Phys. Chem. A* **2004**, *108*, 11151–11159. (b) Bahr, J. L.; Yang, J.; Kosynkin, D. V.; Bronikowski, M. J.; Smalley, R. E; Tour, J. M. *J. Am. Chem. Soc.* **2001**, *123*, 6536–6542. (c) Yao, Z.; Braidy, N.; Botton, G. A.; Adronov, A. *J. Am. Chem. Soc.* **2003**, *125*, 16015–16024.

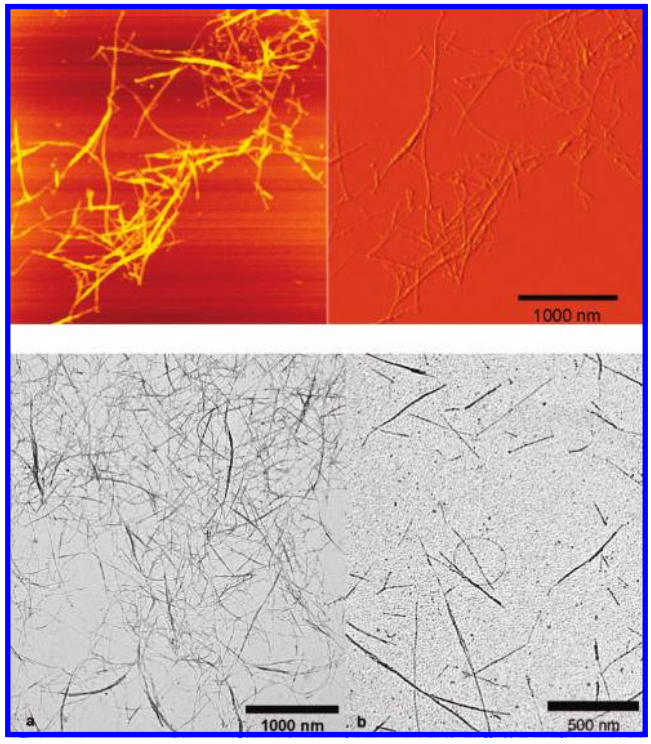

Figure 3. (top) AFM and (bottom) TEM images of SWCNT-*f*-OH.

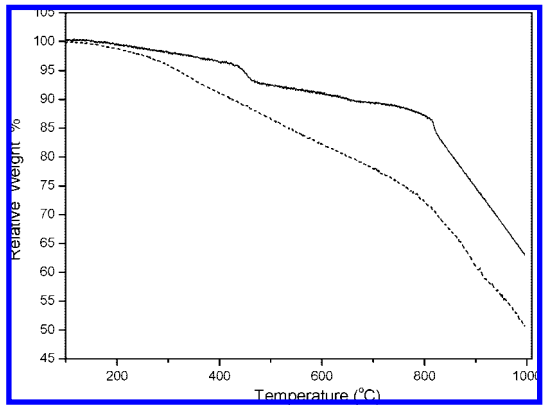

Figure 4. TGA curves of (solid line) pristine SWCNTs and (dashed line) SWCNT-*f*-OH.

from the TEM observations are shown in Figure 3. The images of SWCNT-*f*-OH show that thin bundles of tubes appeared throughout the scanned areas. The lengths of the bundles were on the order of several micrometers, while the diameters ranged from nanometers to micrometers. Comparison of these images with those for the raw material illustrated that debundling took place, providing evidence for the success of the functionalization. AFM characterization (Figure 3) correlated perfectly with what was observed by TEM.

Further evidence for functionalization came from TGA. TGA results for pristine SWCNTs and SWCNT-*f*-OH are shown in Figure 4. SWCNT-*f*-OH exhibited a weight loss of 28% at 800 °C, which roughly corresponds to a functional group every 79 carbon atoms.

The FT-IR spectrum of SWCNT-*f*-OH (Figure 5a) shows C−H stretch features at 2950, 2920, and 2850 cm^{-1} that do not appear in the spectrum of pristine SWCNTs (Figure 5b). Also, apparent C═C stretch bands and a weak aromatic C−H band were observed at 1380−1600 and 3040 cm^{-1}, respectively.

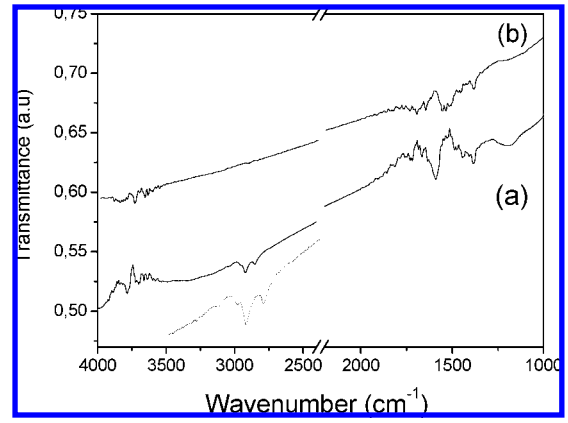

Figure 5. FT-IR spectra of (a) SWCNT-*f*-OH and (b) pristine SWCNTs.

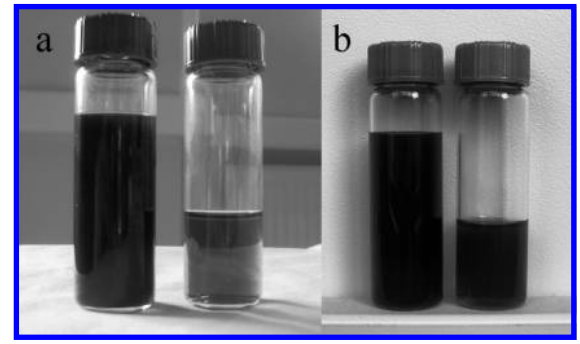

Figure 6. Concentrated and dilute solutions of (a) MWCNT-*f*-OH in ethanol and (b) MWCNT-*f*-ONa in water.

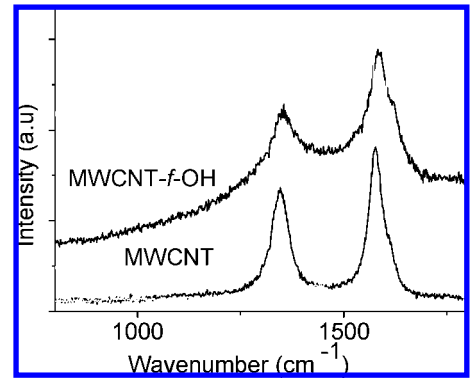

Figure 7. Raman spectra of pristine MWCNTs and MWCNT-*f*-OH.

The C−O stretch band at 1200 cm^{-1} and the O−H stretch band at 3600−3700 cm^{-1}, both of which are characteristic of phenols, were also observed in (Figure 5a), providing additional support for successful functionalization.

Once it was clear that the cycloaddition had proceeded using SWCNTs, the reaction was applied to multiwalled CNTs (MWCNTs). It is easier to work with MWCNTs, as they are less tightly bundled than SWCNTs. Nevertheless, MWCNTs are more difficult to characterize than SWCNTs using typical, limited characterization techniques, and thus, their characterization was achieved using a combination of direct and indirect methods.

In this case, MWCNT-*f*-OH was satisfactorily dispersed in solvents such as ethanol (2 mg mL^{-1}) and DMF (0.4 mg mL^{-1}), providing stable dispersions (Figure 6a). Also, MWCNT-*f*-OH

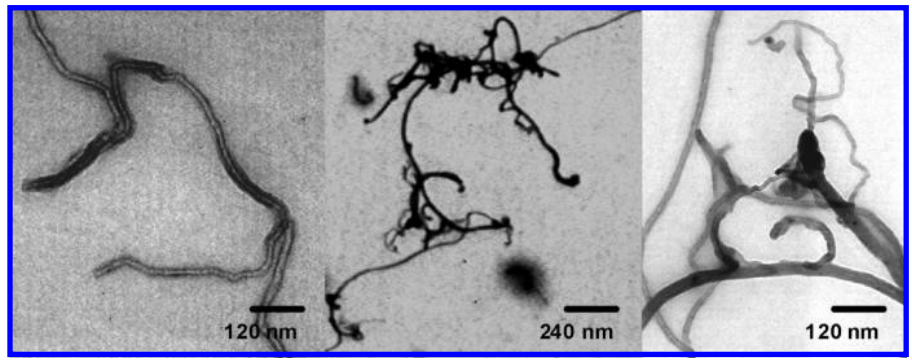

Figure 8. TEM images of MWCNT-*f*-OH.

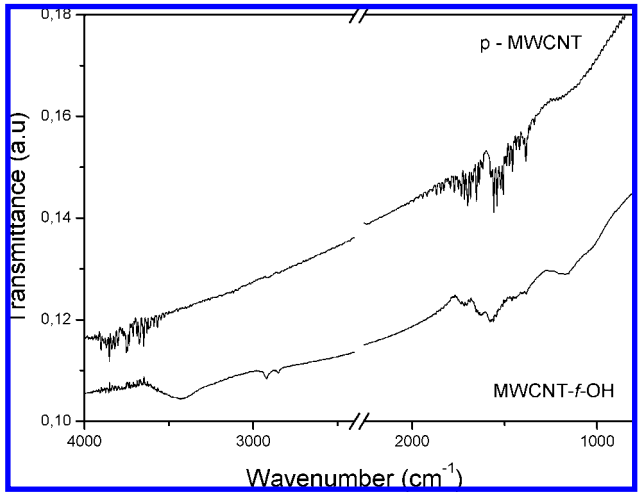

Figure 9. FT-IR spectra of pristine MWCNTs and MWCNT-*f*-OH.

could be easily dispersed at concentrations as high as 0.1 mg mL^{-1} in ethanol/water mixtures with moderate volume ratios. In order to improve the solubility of MWCNT derivatives in water, the hydroxyl groups can be deprotonated in the presence of NaOH to yield the corresponding sodium salts (MWCNT-*f*-ONa); these gave remarkably stable colloidal sols in water (Figure 6b).

Raman spectra showed that the I_G/I_D ratio did not change significantly (Figure 7). This behavior is not unusual for covalently functionalized MWCNTs: the functionalization does not bring any dramatic increment of the sp^3 carbons because it takes place solely on the outer layer. In addition, the D band is partly attributed to amorphous carbon that is removed after reaction. Therefore, any increase in the D-band intensity due to functionalization is more than offset by a simultaneous decrease due to purification.[9]

TEM observations (Figure 8) gave definitive proof of the presence of functionalized MWCNTs in the solutions and mainly showed individual MWCNT-*f*-OH in the scanned area.

As for SWCNT-*f*-OH, the FT-IR spectrum of MWCNT-*f*-OH (Figure 9) shows C−H stretch bands at 2922 and 2853 cm^{-1} that do not appear in the spectrum of pristine MWCNTs. In addition, the presence of the aromatic C═C stretching bands at 1400−1600 cm^{-1} and the C−O stretching band near 1200 cm^{-1} that are characteristic of phenols supports successful functionalization.

An advantage of the phenolic functionalities is that they allow postfunctionalization of the MWCNTs with other molecules that can be employed in preparing customized products. More importantly, the fact that MWCNT-*f*-OH undergoes well-known, established reactions of phenolic groups provides additional proof for successful sidewall functionalization. For instance, silylation of MWCNT-*f*-OH was easily achieved by reaction with hexadecyltrichlorosilane (Scheme 2). MWCNT-*f*-OH was modified by the addition of individual silyl groups as well as oligomeric species[10] formed through C−O−Si covalent bridges, leading to the corresponding hydrophobic adducts. A first indication of the presence of silylated MWCNT-*f*-OH (MWCNT-*f*-OSiR) was provided by the complete loss of the characteristic solubility of MWCNT-*f*-OH in ethanol. The successful reaction was also evidenced by FT-IR spectra (Figure 11) showing the appearance of distinct absorption bands below 3000 cm^{-1}

Scheme 2. Attachment of Hexadecyltrichlorosilane to MWCNT-*f*-OH

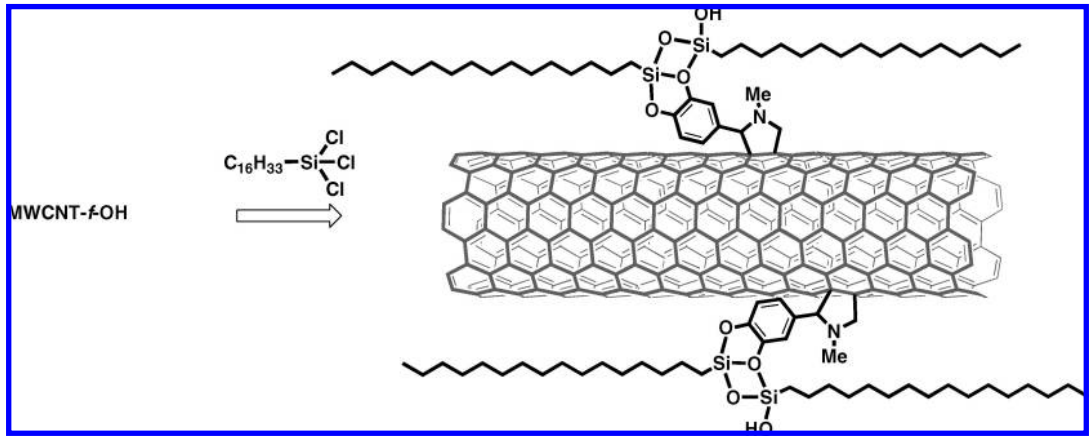

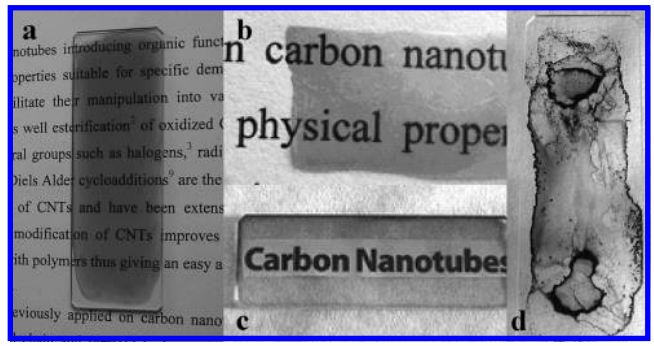

Figure 10. Photographs of optically transparent polymer-composite films obtained by homogeneous dispersion of MWCNT-*f*-OH in (a, b) PAN and (c) EVA polymers. In (b), a free-standing PAN/MWCNT-*f*-OH composite film is presented. (d) Dispersion of pristine MWNTs in PAN, shown for comparison.

Scheme 3. Esterification of MWCNT-*f*-OH Using Trimellitic Anhydride

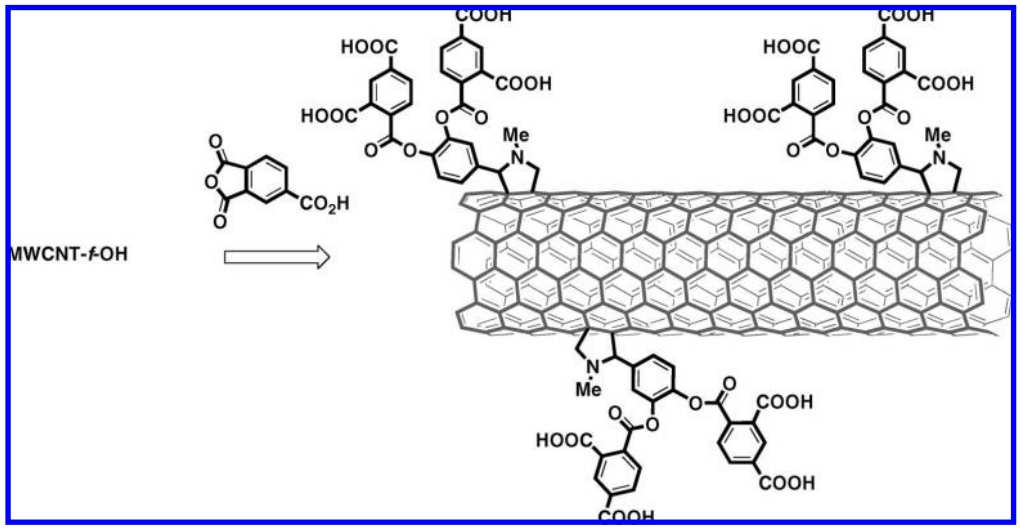

(CH_3- and $-CH_2-$) and at 840 (CH_3-) and 1150 cm^{-1} (Si−O−Si and Si−O−C).

In addition to silylation, a typical reaction of the hydroxyl group is esterification, which was achieved by reaction of MWCNT-*f*-OH with trimellitic anhydride to yield MWCNT-*f*-(ArCOOH) (Scheme 3); this product was not soluble in any solvent. However, in the presence of NaOH, the carboxylic groups were deprotonated, allowing the CNTs to be easily dispersed in water. The success of the functionalization was evidenced by FT-IR spectroscopy (Figure 11): two characteristic absorption bands at 1703 cm^{-1} and 1651 cm^{-1} revealed the presence of carboxylic acid and ester groups, respectively, in MWCNT-*f*-(ArCOOH).

Formation of Composites

Polymer Composites. Polymer nanocomposite research focuses on enhancing the properties of polymers using molecular or nanoscale reinforcements. Polymers have been filled with synthetic and natural compounds to increase tensile strength, modulus, heat and impact resistance, and electrical conductivity. The development of reinforced polymer/CNT composites is difficult because of the problems associated with dispersing pristine CNTs into polymer matrices. Several strategies for overcoming this difficulty have been successfully applied, giving homogeneous polymer/CNT composites that were prepared by

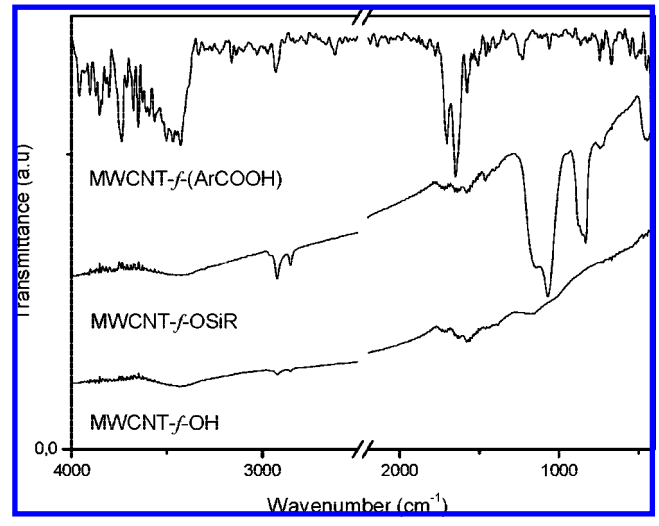

Figure 11. FT-IR spectra of MWCNT-*f*-OH, MWCNT-*f*-OSiR, and MWCNT-*f*-(ArCOOH).

(9) (a) Dang, Z. M.; Wang, L.; Zhang, L. P. *J. Nanomater.* **2006**, 1–5. (b) Wang, L.; Dang, Z. M. *Appl. Phys. Lett.* **2005**, *87*, 1–3. (c) Yang, D. O.; Rochette, J. F.; Sacher, E. *J. Phys. Chem. B* **2005**, *109*, 7788–7794. (d) Li, W.; Zhang, H.; Wang, C.; Zhang, Y.; Xu, L.; Zhu, K.; Xie, S. *Appl. Phys. Lett.* **1997**, *70*, 2684–2686. (e) Huang, W.; Lin, Y.; Taylor, S.; Gaillard, J.; Rao, A. M.; Sun, Y. P. *Nano Lett.* **2002**, *2*, 231–234.
(10) Ma, P. C.; Kim, J. K.; Tang, B. Z. *Carbon* **2006**, *44*, 3232–3238.

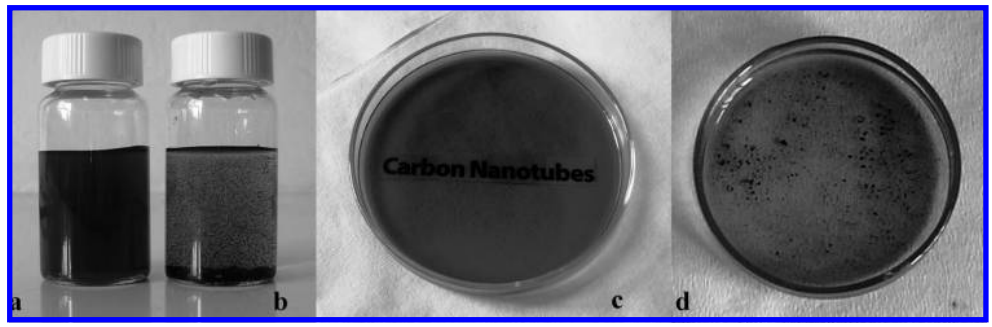

Figure 12. The Laponite/MWCNT-*f*-OH composite formed (a) a stable colloid and, after dilution, (c) an optically transparent dispersion. (b, d) Mixtures of Laponite with pristine MWCNTs showed clear segregation.

Scheme 4. Proposed Adhesion of Laponite Platelets on the Surface of MWCNT-*f*-OH through Its Pendant Phenolic Groups

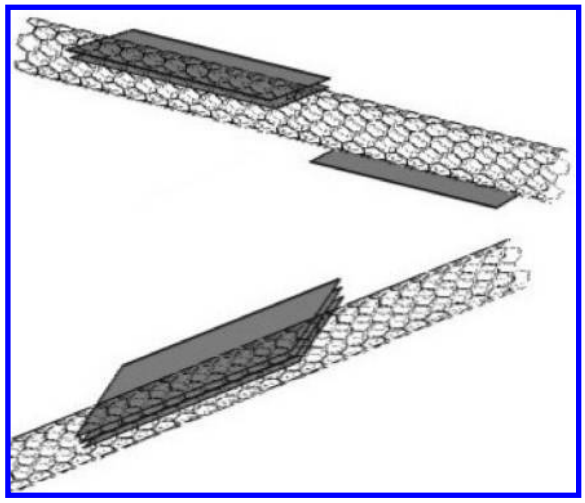

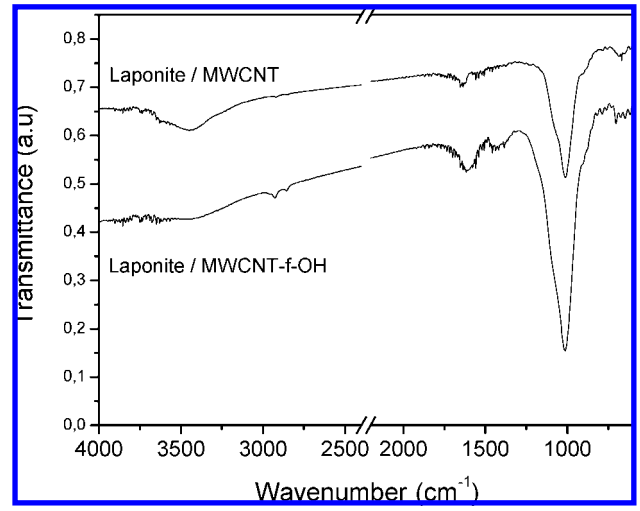

Figure 13. FT-IR spectra of the Laponite/MWCNT-*f*-OH composite and the Laponite/pristine MWCNT mixture.

(i) covalent functionalization of CNTs with polymers[3a] or (ii) in situ polymerization in the presence of CNTs.[3c]

In order to evaluate our OH-functionalized MWCNTs with respect to preparation of composites, we decided to blend MWCNT-*f*-OH with two different types of polymers that have been widely applied and commercialized: (i) polyacrylonitrile (PAN), a resinous or fibrous polymer that is a precursor for high-quality carbon fiber used in sport products, clothes, and concrete reinforcement; and (ii) poly(ethylene vinyl acetate) (EVA), a widely used elastomeric polymer (foam) that has been employed in multiple applications, such as electronics, drug delivery, shock absorption, and encapsulation of silicon cells in the manufacture of photovoltaic modules.

When raw MWCNTs were mixed with PAN or EVA, nonhomogeneous films with clear signs of phase separation were obtained (Figure 10d). In contrast, MWCNT-*f*-OH was uniformly dispersed in the polymer matrix [0.1−2% (w/w)], forming optically transparent, slightly gray films. The films were fabricated by mixing a colloidal dispersion of MWCNT-*f*-OH in DMF with a solution of PAN in DMF. The mixture was spread on a glass slide and allowed to dry, giving a highly homogeneous, transparent gray film (Figure 10a). This film was easily detached from the glass surface (Figure 10b). Similarly, mixing of MWCNT-*f*-OH in DMF with EVA in toluene resulted in uniform, optically transparent films (Figure 10c).

Clay Composites. Other important materials for which demand is increasing are clay minerals, which are widely used in coatings and concrete additives and as composite nanofillers. Clays are naturally occurring materials composed of phyllosilicate minerals; they show plasticity when the amount of water is varied, and they can be hardened when dried. The goal here is to enhance and tailor mechanical and physical properties, such as fire retardancy of the composites. Homogeneous clay/CNT composites have been prepared and studied by (i) in situ growth of CNTs directly on clays,[4a] (ii) mixing of clays and CNTs (with the mediation of epoxy resins),[4c] and (iii) melt blending.[4d]

For our assessment, we chose Laponite, a synthetic layered aluminosilicate mineral, because of its unique combination of colloidal, swelling, intercalation, and ion-exchange properties.[11] We started our research on fabricating composites by adding raw MWCNTs to an aqueous Laponite suspension. The MWCNTs failed to redisperse after the product was dried; the low degree of dispersibility of the raw MWCNTs caused the formation of large aggregates that were easily observed (Figure 12b,d).

An important advantage of MWCNT-*f*-OH is that it forms stable colloids in mixtures of ethanol/water [80:20 (v/v)], which in principle might aid in the fabrication of the composites. The MWCNT-*f*-OH dispersion was mixed with an excess of Laponite [1:10 (w/w)] in water. The presence of clay platelets remarkably enhanced the dispersibility of MWCNT-*f*-OH in water and the stability of the afforded colloids (Figure 12a,c). Moreover, the resulting nanocomposites could be reversibly dried and redispersed in water over many cycles.

(11) Bonn, D.; Kellay, H.; Tanaka, H.; Wegdam, G.; Meunier, J. *Langmuir* **1999**, *15*, 7534–7536.

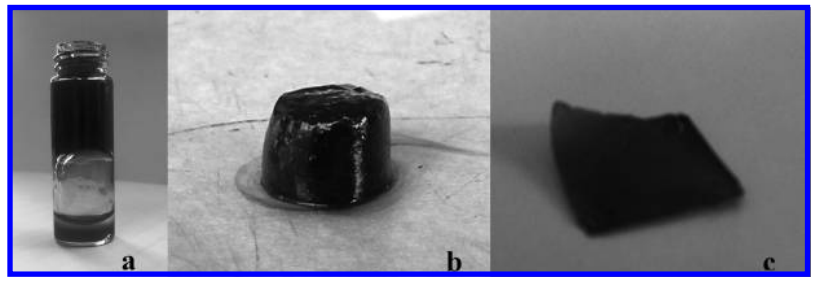

Figure 14. Laponite/MWCNT-*f*-OH composite (a, b) gel and (c) film.

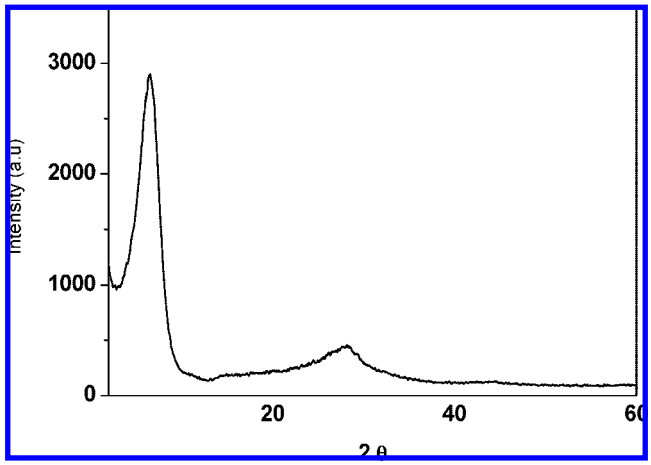

Figure 15. XRD pattern of the Laponite/MWCNT-*f*-OH film.

The enhanced solubility of MWCNT-*f*-OH in the presence of Laponite can be attributed to interactions between the phenol functionalities of MWCNT-*f*-OH and the hydroxyl groups (e.g., from defect sites) of individual Laponite platelets (Scheme 4). Consequently, the increased dispersibility of MWCNT-*f*-OH in water results from the ionic character of the Laponite sheets that stick on their surface. As a matter of fact, it is well-established that charged nanoparticles or clusters attached to the surfaces of uncharged particles can impart colloidal stability under the dominance of segregative Coulombic repulsions.[12]

Comparison of the FT-IR spectra of the Laponite/MWCNT-*f*-OH composite and the Laponite/pristine MWCNT mixture demonstrates the enhancement of compatibility obtained by use of MWCNT-*f*-OH (Figure 13). The spectrum of the Laponite/MWCNT-*f*-OH composite shows a strong band at 1020 cm^{-1} due to the Si−O stretch in Laponite as well as the bands at 2920, 2850, 1400, and 1600 cm^{-1} characteristic of the functionalized MWCNTs (see Figure 9). In contrast, the presence of MWCNTs is less evident in the spectrum of the Laponite/pristine MWCNT mixture due to the lack of intense bands for pristine MWCNTs and their low dispersability among the Laponite platelets. Thus, only the characteristic Si−O−Si band at 1020 cm^{-1} and the bands at 3400 and 1640 cm^{-1} from absorbed water were recorded.

Furthermore, more-concentrated Laponite/MWCNT-*f*-OH colloids formed composite gels that showed no signs of phase separation (Figure 14a,b). The adhered Laponite sheets provide MWCNT-*f*-OH with ion-exchange properties, thereby potentially enabling the immobilization of various cationic species having specific functions (dyes, drugs, biomolecules, or polyelectrolytes). A notable finding was the fabrication of self-supported, monolithic composite films by casting (Figure 14c). Laponite and its intercalated derivatives generally form shattered films upon drop-casting and drying. Nevertheless, addition of a small amount of fibrous MWCNT-*f*-OH binds the Laponite platelets together, thereby leading to coherent films that are free of cracks.

The films were further characterized using X-ray diffraction (XRD) in order to obtain additional information about the structure and morphology of the resulting nanocomposite. The XRD pattern of the film (Figure 15) shows a well-defined reflection attributed to the Laponite prime particles ($d_{001} \approx 13$ Å). Since no interlayer space expansion occurred, we can conclude that either the functionalized nanotubes were located at the external surface of the clay particles or that the CNTs were covered with packages of clay platelets consisting of a few clay layers stacked in perfect registry with maintained order (lamination).

Conclusions

We have shown that covalent functionalization of CNTs with phenol groups via 1,3-dipolar cycloaddition is a powerful tool for enhancing the solubility of CNTs in polar solvents, including DMF, ethanol, and water. The colloidal state of MWCNT-*f*-OH dispersions facilitates processing of the CNTs and increases their compatibility with other components such as polymers and clays. The fabrication of homogeneous, coherent, transparent CNT composite films and/or gels was achieved by simple mixing colloidal solutions of CNTs with solutions of polymers or clays without the need for more sophisticated fabrication techniques such as in situ polymerization or melt blending.

Experimental Section

Physical Measurements. Raman spectra over the range 1000−2400 cm^{-1} were recorded with a Renishaw RM 1000 Micro-Raman system using a Nd:YAG laser excitation line at 532 nm. A power of 0.5−1 mW and 1 μm focus spot were used in order to avoid photodecomposition of the samples.

TEM was carried out on a JEOL JEM 2010 microscope operated at 200 kV (LaB_6 cathode, point resolution 1.94 Å). The images presented here are typical and representative of the samples under observation.

AFM measurements on samples deposited from DMF solutions by spin coating (3000 rpm × 3 min) onto silicon wafers were carried out on a Digital Instruments (Veeco) Nanoscope IIIa using Veeco RTESP5 tips.

FT-IR spectra over the range 400−4000 cm^{-1} were measured with a Bruker EQUINOX 55S infrared spectrometer equipped with a deuterated triglycine sulfate detector. Each spectrum was the

(12) (a) Tohver, V.; Chan, A.; Sakurada, O.; Lewis, J. A. *Langmuir* **2001**, *17*, 8414–8421. (b) Bourlinos, A. B.; Georgakilas, V.; Zboril, R.; Dallas, P. *Carbon* **2007**, *45*, 2136–2139. (c) Bourlinos, A. B.; Bakandritsos, A.; Zboril, R.; Karakassides, M.; Trapalis, C. *Carbon* **2007**, *45*, 1108–1111. (d) Garrigue, P.; Delville, M. H.; Labrugère, C.; Cloutet, E.; Kulesza, P. J.; Morand, J. P.; Kuhn, A. *Chem. Mater.* **2004**, *16*, 2984–2986.

average of 64 scans collected at a resolution of 2 cm^{-1}. Samples were in the form of KBr pellets containing 2 wt % sample material.

XRD patterns were recorded on a Siemens XD-500 diffractometer using Cu Kα radiation. The patterns were recorded over a 2θ range of 2−100° in steps of 0.02° with a counting time of 2 s per step. Samples were in the form of films supported on glass substrates.

Synthetic Procedures. SWCNT-*f*-OH. Twenty milligrams of HiPCo SWCNTs (Carbon Nanotechnologies, batch R0510C), 200 mg of 3,4-dihydroxybenzaldehyde, and 200 mg of *N*-methylglycine were suspended in 50 mL of DMF and heated at 120 °C for 5 days. The mixture was then filtered through Millipore filters (0.45 μm FG) and washed thoroughly with DMF. The filtrate was sonicated in DMF for 1 h and then removed; the resulting suspension was filtered again through Millipore filters (0.45 μm FG). This procedure was repeated three additional times with sonication in (1) DMF, (2) 1:1 (v/v) ethanol/$CHCl_3$, and (3) diethyl ether. The remaining black solid was dried under vacuum (10^{-2} bar) for 3 days.

MWCNT-*f*-OH. Twenty milligrams of pristine MWCNTs (Aldrich), 200 mg of 3,4-dihydroxybenzaldehyde, and 200 mg of *N*-methylglycine were suspended in 50 mL of DMF. The mixture was heated at 120 °C for 5 days, and the solid part was separated by centrifugation (3500 rpm, 5 min) and washed with DMF (1 × 20 mL) and acetone (2 × 20 mL) to remove unreacted organics. The purified product was dispersed in 100 mL of ethanol and filtered off. The ethanol dispersion was concentrated to dryness to give a black solid.

MWCNT-*f*-OSiR. MWCNT-*f*-OH (10 mg) and hexadecyltrichlorosilane (0.5 mL) were refluxed overnight in toluene (20 mL). The product was isolated by centrifugation and washed several times with toluene.

MWCNT-*f*-(ArCOOH). MWCNT-*f*-OH (10 mg) and trimellitic anhydride (50 mg) were stirred overnight at room temperature in DMF (20 mL). The resulting product was isolated by centrifugation and washed with acetone.

PAN/MWCNT-*f*-OH. MWCNT-*f*-OH (0.1−2 mg) dispersed in ethanol was added slowly to a solution of 100 mg of PAN in 10 mL of hot DMF. The mixture was heated at 110 °C to remove ethanol. The remaining solution was spread on a glass slide and formed a film upon air-drying.

EVA/MWCNT-*f*-OH. MWCNT-*f*-OH (0.1−2 mg) dispersed in ethanol was added slowly to a solution of 100 mg of EVA in 10 mL of hot toluene. The solution was spread on a glass slide and formed a uniform film upon air-drying.

Laponite/MWCNT-*f*-OH. Laponite (100 mg) was dispersed in 10 mL of distilled water after overnight stirring. MWCNT-*f*-OH (2−30 mg) dispersed in 4−10 mL of 80:20 (v/v) ethanol/water was added slowly to the Laponite dispersion and stirred overnight. The mixture was air-dried on a glass plate or kept as a dispersion over several weeks.

Acknowledgment. A.M.-A. and M.P. acknowledge partial support from EU network EMMMA, Università di Trieste, Giovani Ricercatori Program (UNITS), INSTM, and MUR (PRIN 2006, Prot. 2006034372, and FIRB, Prot. RBNE033KMA). This work was supported in part by the General Secretariat of Research and Technology of Greece through the PENED 2003 program (03ED 548). Mr. Claudio Gamboz (Centro Servizi Polivalenti di Ateneo, Università di Trieste) is gratefully acknowledged for assistance with TEM imaging. We are grateful to Mr. Daniel Peitz for the picture shown in Scheme 1.

JA8002952